International Journal of Automotive Technology, Vol. 17, No. 6, pp. 1091–1100 (2016)
DOI 10.1007/s12239–016–0106–x

pISSN 1229–9138/ eISSN 1976–3832

MODEL-INDEPENDENT SELF-TUNING FAULT-TOLERANT CONTROL METHOD FOR 4WID EV

Y. LUO*, J. LUO and Z. QIN

State Key Laboratory of Automotive Safety and Energy, Tsinghua University, Beijing 100084, China

(Received 5 August 2015; Revised 9 April 2016; Accepted 13 May 2016)

ABSTRACT–To solve the problem of the existing fault-tolerant control system of four-wheel independent drive (4WID) electric vehicles (EV), which relies on fault diagnosis information and has limited response to failure modes, a model-independent self-tuning fault-tolerant control method is proposed. The method applies model-independent adaptive control theory for the self-tuning active fault-tolerant control of a vehicle system. With the nonlinear properties of the adaptive control, the complex and nonlinear issues of a vehicle system model can be solved. Besides, using the online parameter identification properties, the requirement of accurate diagnosis information is relaxed. No detailed model is required for the controller, thereby simplifying the development of the controller. The system robustness is improved by the error based method, and the error convergence and input-output bounds are proved via stability analysis. The simulation and experimental results demonstrate that the proposed fault-tolerant control method can improve the vehicle safety and enhance the longitudinal and lateral tracking ability under different failure conditions.

KEY WORDS : Fault-tolerant control, Four-wheel independent drive electric vehicles, Model-independent adaptive control, Multiple actuators fault

NOMENCLATURE

4WID : four wheel independent drive
EV : electric vehicle
HEV : hybrid electric vehicle
MIMO : multiple input multiple output
BIBO : bounded input bounded output

1. INTRODUCTION

Multiple actuators fault-tolerant control of 4WID EV uses a redundant actuator configuration to ensure that the vehicle tracks the driver's intention when one or more wheel motors degrade or even shut down. The coordination of redundant actuators improves the safety performance of 4WID EV and fulfills the vehicle longitudinal and lateral control targets.

Fault-tolerant control was first used in the aviation and aerospace industries, and many control methods were used, including linear quadratic control (Yang *et al.*, 2000; Veillette, 1995), control allocation (Aiwi and Edwards, 2008), sliding mode control (Hess and Wells, 2003; Kazemi and Janbakhsh, 2010), machine learning (Ho and Yen, 2002; Polycarpou, 2001), and so on. In vehicle fault-tolerant control areas, most researches aimed at x-by-wire systems (Gadda *et al*., 2007; Im *et al*., 2009). Currently, the fault-tolerant control on electric vehicle drive systems focused more on motor fault diagnosis (Wang and Wang, 2011; Widodo *et al*., 2009) and failure response (Benbouzid *et al*., 2007; Wang and Wang, 2013). However, these studies had not paid much attention to the fault-tolerant control methods of electric vehicles.

Kawakami *et al*. (2001) proposed to shut down the failing drive wheel and the drive wheel on the opposite side; this method may provide a portion of the traction for the cases of one wheel failure or coaxial two wheels failure, and the control logic was easy to implement. Zidani *et al*. (2003) introduced an intelligent control method which could improve the performance of the fault-tolerant control for EVs or HEVs. Two control methods were used, sliding mode for encoder-based control; and fuzzy logics for sensorless control. The system control reorganization can improve the transitions smoothness. Plumlee and Bevly (2004) proposed a control allocation method based on quadratic programming for vehicle yaw motion tracking. Wang and Longoria (2009) discussed the method of using control allocation to address the over-actuated system; the basic idea is to establish a control effectiveness matrix, resulting in the corresponding control parameters. Yim (2014) presented a fault-tolerant yaw moment control for a vehicle with steer-by-wire and brake-by-wire devices, which can realize active front steering and electronic stability control functions that is effective for failure safety. Wada *et al*. (2013) proposed a synthesis method for a reconfigurable fault-tolerant control system in a steer-by-wire vehicle, which utilized a control allocator based on

**Corresponding author.* e-mail: lyg@tsinghua.edu.cn

on-line optimization. The control method can guarantee the stability of the overall system.

Active fault-tolerant control considers the implementation of the partial failure situation, as opposed to passive fault-tolerant control. However, almost all of these methods are model-based, in which the modeling and solving of such models is complex and is strongly dependent on the fault diagnosis system.

Adaptive fault-tolerant control which is independent of the fault diagnosis system can solve the problems preferably, but the existing research primarily focuses on the aviation and aerospace field. MacKunis *et al*. (2010) developed an unmanned aerial vehicle which utilized an adaptive method to compensate for the parametric uncertainty. Wise *et al*. (1999) presented a direct adaptive reconfigurable flight control approach of an advanced tailless fighter aircraft. Kim *et al*. (2003) proposed a control method using a model following controller with direct adaptive update rules to realize better performance of reconfigurable flight control. However, adaptive fault-tolerant control has rarely been used on automotive systems. Besides, it will be more beneficial when the control method is used on 4WID EVs.

To address the limitations of these previous studies, a model-independent self-tuning fault-tolerant control method for 4WID EV is proposed in this study. This active fault-tolerant control method is developed based on model-independent adaptive control theory, which does not rely on a detailed model or the diagnosis system. So there are two advantages of the proposed method: (1) Using the nonlinear characteristics of the adaptive control, the method can eliminate the complexity and nonlinearity of the vehicle system model, which will reduce the amount of computation greatly. (2) The use of online parameter identification (mainly index matrix between input and output) reduces the requirement for accurate diagnostic information of the multi-actuator fault diagnosis system. The paper is organized as follows. The model-independent self-tuning fault-tolerant control method is developed in Section 2. The error convergence and the bounded input and bounded output stability are demonstrated in section 3. Simulations and experiments are performed to validate the control method in Sections 4 and 5. Conclusions are given in Section 6.

2. MODEL-INDEPENDENT SELF-TUNING FAULT-TOLERANT CONTROL METHOD

2.1. Vehicle Model Including the Actuator Failure

The vehicle model is the basis of the fault-tolerant control; although the control referred to here is model-independent control, it does not mean that no vehicle model is used. A vehicle model is necessary to determine the basic input-output controller and the vehicle restraint system.

The discrete non-linear vehicle system will be described as the following MIMO system:

$$\begin{aligned}&\boldsymbol{y}(k+1)=\\&f(\boldsymbol{y}(k),\ldots,\boldsymbol{y}(k-n_{\mathrm{y}}),\boldsymbol{u}(k),\ldots,\boldsymbol{u}(k-n_{\mathrm{u}}))\end{aligned}\tag{1}$$

The system input and output is:

$$\boldsymbol{u}(k)=[T_{\mathrm{fl}}(k),T_{\mathrm{fr}}(k),T_{\mathrm{rl}}(k),T_{\mathrm{rr}}(k),T_{\mathrm{s}}(k)]^{\mathrm{T}}\tag{2}$$

$$\boldsymbol{y}(k)=(\omega_{\mathrm{fl}}(k),\omega_{\mathrm{fr}}(k),\omega_{\mathrm{rl}}(k),\omega_{\mathrm{rr}}(k),\delta_{\mathrm{f}}(k))^{\mathrm{T}}\tag{3}$$

Where $\boldsymbol{u}(k)$ and $\boldsymbol{y}(k)$ is the system input and output, respectively, at time k; $T_{\mathrm{fl}}(k)$, $T_{\mathrm{fr}}(k)$, $T_{\mathrm{rl}}(k)$, $T_{\mathrm{rr}}(k)$ are the wheel torques of the four wheels; and $T_{\mathrm{s}}(k)$ is the steering torque. $\omega_{\mathrm{fl}}(k)$, $\omega_{\mathrm{fr}}(k)$, $\omega_{\mathrm{rl}}(k)$, $\omega_{\mathrm{rr}}(k)$ are the wheel speeds and $\delta_{\mathrm{f}}(k)$ is the steering angle. $f(\cdots)$ is a nonlinear function. Considering the above nonlinear system, the failure factor ζ is introduced when a fault occurs. In this study, actuator failure, especially the motor failure, is of concern. When the motor fails, it cannot provide drive torque or the torque provided is limited. To describe the implementation capability of the actuator after failure, the failure factor ζ is defined as:

$$\zeta=\begin{cases}1 & Normal\\ 0\sim 1 & Partial\ \ Failure\\ 0 & Shut\ \ down\end{cases}\tag{4}$$

ζ describes the extent of the actuator failure; the smaller the factor ζ is, the more severe the failure is. When the failure factor $\zeta=1$, the actuator is working properly; when the failure factor $\zeta=0$, the actuator completely loses the ability to actuate; and when failure factor satisfies $0<\zeta<1$, the actuator is in partial failure, with some ability to execute. In a conventional fault-tolerant control system, the value ζ is given by the fault diagnosis system; however, diagnostic systems are usually very complex systems.

Using the failure factor defined by formula (4), the actual actuation capacity can be described by varying degrees of failure of the drive system:

$$T_{(\cdot)}=\begin{cases}T_{(\cdot)} & Normal\\ \zeta T_{(\cdot)} & Partial\ \ Failure(0<\zeta<1)\\ 0 & Shut\ \ down\end{cases}\tag{5}$$

$(\cdot)$ represents front left, front right, rear left, or rear right. The input can be written as:

$$\boldsymbol{u}(k)=\boldsymbol{u}_{\zeta}(k)\tag{6}$$

Wherein, $\boldsymbol{u}_{\zeta}(k)=\boldsymbol{\zeta}(k)\boldsymbol{u}(k)$, and the description of the system failure becomes:

$$\begin{aligned}&\boldsymbol{y}(k+1)=\\&f(\boldsymbol{y}(k),\ldots,\boldsymbol{y}(k-n_{y}),\boldsymbol{u}_{\zeta}(k),\ldots,\boldsymbol{u}_{\zeta}(k-n_{\mathrm{u}}))\end{aligned}\tag{7}$$

2.2. Self-tuning Fault-tolerant Controller

For discrete-time nonlinear Multi-Input Multi-Output (MIMO) systems, model-independent adaptive control theory is used to construct a fault-tolerant controller for a

discrete-time nonlinear MIMO system. The controller uses the dynamic linearization method (Hou and Jin, 2011), which fulfills the online input and output data estimates based on the equivalent data model and the pseudo-Jacobian matrix of the controlled system operating point to construct the response item; the experience coefficient and the error integral are utilized as the holding item. By combining the holding item and response item, the controller becomes:

$$\boldsymbol{u}_{\zeta}(k) = \boldsymbol{u}_{\zeta}(k-1) + \hat{\boldsymbol{Z}}_{\text{res}} + \hat{\boldsymbol{Z}}_{\text{con}} \tag{8}$$

Where $\hat{\boldsymbol{Z}}_{\text{res}}$ represents the response item and $\hat{\boldsymbol{Z}}_{\text{con}}$ represents the holding item.

$$\hat{\boldsymbol{Z}}_{\text{res}} = \frac{z_{2\_d}\boldsymbol{J}_{\text{p}}^{\text{T}}(k)(\boldsymbol{y}_{\text{ref}}(k+1) - \boldsymbol{y}(k))}{z_{1\_d} + \left\|\boldsymbol{J}_{\text{p}}(k)\right\|^2} \tag{9}$$

where z_{1_d} and z_{2_d} are experience values and the estimated $\boldsymbol{J}_{\text{p}}(k)$ values are:

$$\hat{\boldsymbol{J}}_{\text{p}}(k) = \hat{\boldsymbol{J}}_{\text{p}}(k-1) + \frac{z_{4\_d}((\Delta\boldsymbol{y}(k) - \hat{\boldsymbol{J}}_{\text{p}}(k-1)\Delta\boldsymbol{u}_{\zeta}(k-1))(\Delta\boldsymbol{u}_{\zeta}(k-1))^{\text{T}})}{z_{3\_d} + \left\|\Delta\boldsymbol{u}_{\zeta}(k-1)\right\|^2} \tag{10}$$

where z_{3_d} is the weighting factor for limiting the excessive variation in the pseudo-Jacobian estimation matrix, $z_{3\_d} > 0$. z_{4_d} is a step size factor, and $0 < z_{4\_d} \leq 2$.

$$\hat{\boldsymbol{Z}}_{\text{con}} = z_{5\_d}\hat{\boldsymbol{K}} \tag{11}$$

z_{5_d} represents the experience value and $z_{5\_d} > 0$. $\hat{K}$ is the key estimated value of the holding item, the derivative is given by formula (12).

$$\dot{\hat{\boldsymbol{K}}} = \boldsymbol{y}_{\text{ref}}(k+1) - \boldsymbol{y}(k) \tag{12}$$

2.3. Failure Modes for 4WID EV

For 4WID EV, four drive motors are located in the four wheels (or besides the wheels). Depending on the location and the number of motor failures which means the motor has a loss-of-effectiveness fault or the motor stops working, six types of failure modes can be concluded: single motor failure, two motors failing at the same side, two motors failing on the same shaft, two motors failing on different shaft and opposite side, three-motor failure, and four-motor failure.

2.3.1. Single motor failure

When single motor failure occurs, there are two degrees of freedom for the longitudinal and lateral force control (limited to the drive motor system); the loss of the longitudinal force can be compensated by the remaining motors' drive force, and the lateral error can either be eliminated by driving force reallocation or be eliminated by steering compensation.

2.3.2. Two motors failing at the same side

When two motors at the same side fail, there is only one degree of freedom for the longitudinal and lateral force control. The loss of longitudinal force can be compensated within a certain range by the remaining motors' drive power, but the lateral disturbance cannot be eliminated through the redistribution of drive force. At this time, steering control can be used to solve the problem.

Previous studies used only the driving force distribution; in this study, active steering is used to compensate for the yaw rate disturbance, which has a wider range of adaptability.

2.3.3. Two motors failing on the same shaft

When two coaxial motors fail, for the longitudinal and lateral force control, there are two degrees of freedom; the loss of longitudinal force can be compensated by the remaining drive power, and the lateral error is not obvious.

2.3.4. Two motors failing on different shafts and opposite sides

When two motors on different shafts and opposite side fail, for the longitudinal and lateral force control, there are two degrees of freedom, and the loss of longitudinal force can be compensated by the remaining motor drive power within a certain range; the lateral error is also not obvious.

2.3.5. Three-motor failure

Under the cases of three-motor failure, for the control variables of the longitudinal and lateral forces, there is only one degree of freedom, the loss of the longitudinal force is often difficult to compensate by the remaining motor power, and vehicles can only move slowly; lateral error can be compensated by steering control.

2.3.6. Four-motor failure

Under the cases of four-motor failure, for partial failure, the longitudinal and lateral forces may exhibit some degrees of freedom, but during shutdown, the vehicle cannot continue traveling.

In summary, there are a total of 16 types of failure modes; according to the severity of the failure, they can be divided into the controllable and uncontrollable failure.

(1) The controllable failure is the failure when a fault occurs; through the coordination of the remaining actuators, vehicle tracking can still be guaranteed to the level of the expectations.
(2) The uncontrollable failure is the failure when a fault occurs; through the coordination of the remaining actuators, vehicle tracking can't be guaranteed.

2.4. Fault-tolerant Control System of the Controllable Failure

This section addresses the controllable failure by using the self-tuning fault-tolerant controller described in Section 2.2. Applying the above theory to the vehicle system, the input and output remains unchanged. The vehicle system is a physical system; the input should be constrained by the

physical environment and the specific conditions.

2.4.1. Constraint of the steering system

This paper only considers the use of steering to correct yaw rate deviation; when driving straight, if two wheel motors at the same side fail while the speed limit is reached, then the maximum yaw rate deviation appears. Formula (13) indicates the need to control the bias correcting steering angle:

$$\Delta\delta_{\mathrm{f}} = \frac{\Delta\dot{\psi}(a+b)(1+Kv_{\mathrm{x}}^2)}{v_{\mathrm{x}}} \tag{13}$$

Set the speed $v_{x\max}$ = 120 km/h, and then simulate the fault state to achieve the maximum deviation of the yaw rate. The yaw rate data $\Delta\psi_{\max}$ obtained from the simulation are + 1.65 °/s and −1.65 °/s, resulting in the steering angle $\Delta\delta_{\mathrm{fmax}}$ = ± 7°. This steering angle is the maximum front-wheel active steering angle corresponding to an intervention; steering angles greater than this value indicate that the calculation is unreasonable and may cause vehicle instability, that is, the designed steer angle constraint is:

$$\left|\Delta\delta_{\mathrm{f}}\right| \le \left|\Delta\delta_{\mathrm{f\,max}}\right| \tag{14}$$

2.4.2. Constraints of the motor capacity and increment

When fulfilling tolerant control, the motor capacity constraints must be considered to protect the motor and maintain the vehicle under good working conditions. Using brushless DC hub motor as an example, the motor capacity and incremental constraints are considered.

For a brushless DC motor, the motor torque relevant with the rotational speed constraints is:

$$T_{(\cdot)} \le T_{(\cdot)\max} = f(n) \tag{15}$$

Drive motors not only serve fault-tolerant control but also serve in the normal traveling as a source of power. When motors enter a fault-tolerant mode, the other motors normally operate for a certain time or even under a large working load; at this time, the motor temperature plays a dominant role. As a result, according to the experimental peak torque and temperature relationships formula, the designed available torque to achieve motor overload constraints is:

$$T_{(\cdot)} \le T_{(\cdot)\max} = f(t_{\mathrm{c\_iwm}}) \tag{16}$$

In which $t_{\mathrm{c\_twm}}$ is the hub motor armature temperature and the torque can be determined via a temperature curve.

The rapid change of the motor torque improves the vehicle response; however, it will also cause mechanical shock and comfort issues, and even affect the motor's life. Therefore, to protect the motor, increments of the constraints of the motor torque are required.

$$\dot{T}_{(\cdot)} \le cr_{\max} \tag{17}$$

where $cr_{\max}$ is the maximum allowable rate of change of the motor torque. Chang the formula (17) into linear constraints:

$$T_{(\cdot)} \le T_{(\cdot)}(t-\Delta t) + cr_{\max}\Delta t \tag{18}$$

Δt is the step size.

In summary, the self-tuning fault-tolerant control system considering all constraints is as follows:

$$\begin{aligned}&\boldsymbol{u}_{\zeta}(k) = \boldsymbol{u}_{\zeta}(k-1)\\&+\frac{z_{2\_\mathrm{d}}\boldsymbol{J}_{\mathrm{p}}^{\mathrm{T}}(k)(\boldsymbol{y}_{\mathrm{ref}}(k+1)-\boldsymbol{y}(k))}{z_{1\_\mathrm{d}}+\left\|\boldsymbol{J}_{\mathrm{p}}(k)\right\|^2}+z_{5\_\mathrm{d}}\hat{\boldsymbol{K}}\end{aligned} \tag{19}$$

Subject to: Formulas (14) ~ (16) and Formula (18).

3. STABILITY ANALYSIS

To prove the system stability of the fault-tolerant control, tracking errors convergence as well as input and output bounds (Bounded-Input Bounded-Output, BIBO) is required.

3.1. Error Sequence Convergence Proof

The system output error is defined as:

$$\boldsymbol{e}(k) = \boldsymbol{y}_{\mathrm{ref}} - \boldsymbol{y}(k) \tag{20}$$

Substitution of the tight format linear dynamic data model $\Delta\boldsymbol{y}(k+1) = \boldsymbol{J}_{\mathrm{p}}(k)(\Delta\boldsymbol{u}_{\zeta}(k))$ and the control algorithm $\boldsymbol{u}_{\zeta}(k) = \boldsymbol{u}_{\zeta}(k-1) + \hat{\boldsymbol{Z}}_{\mathrm{res}}$ into Formula (20), we have:

$$\begin{aligned}&\boldsymbol{e}(k+1) = \boldsymbol{e}(k) - \boldsymbol{J}_{\mathrm{p}}(k)\Delta\boldsymbol{u}_{\zeta}(k)\\&=\left[\boldsymbol{I}-\frac{z_{2\_\mathrm{d}}\boldsymbol{J}_{\mathrm{p}}(k)\hat{\boldsymbol{J}}_{\mathrm{p}}^{\mathrm{T}}(k)}{z_{1\_\mathrm{d}}+\left\|\hat{\boldsymbol{J}}_{\mathrm{p}}(k)\right\|^2}\right]\boldsymbol{e}(k)\end{aligned} \tag{21}$$

From the conclusion of the spectral radius (Wang and Wang, 2013), there exists an arbitrarily small positive number ε_1 such that:

$$\begin{aligned}&\left\|I-\frac{z_{2\_\mathrm{d}}\boldsymbol{J}_{\mathrm{p}}(k)\hat{\boldsymbol{J}}_{\mathrm{p}}^{\mathrm{T}}(k)}{z_{1\_\mathrm{d}}+\left\|\hat{\boldsymbol{J}}_{\mathrm{p}}(k)\right\|^2}\right\|_{\mathrm{v}}\\&<s\left(\boldsymbol{I}-\frac{z_{2\_\mathrm{d}}\boldsymbol{J}_{\mathrm{p}}(k)\hat{\boldsymbol{J}}_{\mathrm{p}}^{\mathrm{T}}(k)}{z_{1\_\mathrm{d}}+\left\|\hat{\boldsymbol{J}}_{\mathrm{p}}(k)\right\|^2}\right)+\varepsilon_1<1\end{aligned} \tag{22}$$

In which $\|*\|_v$ is the compatible norm with the matrix (*).

Taking the norm on both sides of the Formula (21), we have:

$$\left\|\boldsymbol{e}(k+1)\right\|_{\mathrm{v}} \le \left\|\boldsymbol{I}-\frac{z_{2\_\mathrm{d}}\boldsymbol{J}_{\mathrm{p}}(k)\hat{\boldsymbol{J}}_{\mathrm{p}}^{\mathrm{T}}(k)}{z_{1\_\mathrm{d}}+\left\|\hat{\boldsymbol{J}}_{\mathrm{p}}(k)\right\|^2}\right\|\left\|\boldsymbol{e}(k)\right\|_{\mathrm{v}} \le \left\|\boldsymbol{e}(k)\right\|_{\mathrm{v}} \tag{23}$$

By Formula (23), the tracking error sequence convergence is obtained.

3.2. BIBO Proof

In the output error definition, as $\boldsymbol{y}_{\mathrm{ref}}$ is a given constant vector and $\boldsymbol{e}(k)$ is bounded, the output $\boldsymbol{y}(k)$ is bounded.

Because $\hat{\boldsymbol{J}}_{\mathrm{p}}(k)$ is bounded (Hou and Jin, 2011), there is always such a positive number M that the following formula is established:

$$\left\| \frac{z_{2\_\mathrm{d}} \hat{\boldsymbol{J}}_{\mathrm{p}}^{\mathrm{T}}(k)}{z_{1\_\mathrm{d}} + \left\| \hat{\boldsymbol{J}}_{\mathrm{p}}(k) \right\|^2} \right\|_{\mathrm{v}} \leq M \tag{24}$$

Using formula $\boldsymbol{u}_{\zeta}(k) = \boldsymbol{u}_{\zeta}(k-1) + \hat{\boldsymbol{Z}}_{\mathrm{res}}$, Formulas (23) and (24) can be derived:

$$\left\| \boldsymbol{u}_{\zeta}(k) \right\|_{\mathrm{v}} \leq M \left\| \boldsymbol{e}(1) \right\| \tag{25}$$

That means $\boldsymbol{u}_{\zeta}(k) = \boldsymbol{u}_{\zeta}(k-1) + \hat{\boldsymbol{Z}}_{\mathrm{res}}$ is bounded; besides, because the error tends to 0, $\hat{\boldsymbol{Z}}_{\mathrm{con}}$ must be bounded stable, the input $\boldsymbol{u}_{\zeta\mathrm{c}}(k) = \boldsymbol{u}_{\zeta\mathrm{c}}(k-1) + \hat{\boldsymbol{Z}}_{\mathrm{res}} + \hat{\boldsymbol{Z}}_{\mathrm{con}}$ being bounded is proved. Thus, the closed-loop system is BIBO stable.

4. SIMULATION AND ANALYSIS

The proposed fault-tolerant control method is validated by a simulation system based on Simulink and CarSim, which is shown in Figure 1. The independent driving system, the electric controlled steering system, the driving and braking torque controller and the model-independent self-tuning fault-tolerant controller are developed in Simulink respectively. A basic A-class sedan vehicle model of Carsim is chosen for the simulation. The main parameters of the vehicle, including actuator systems, are presented in Table 1. In order to compare with the experiment results, all the parameters of the simulation except for the maximum motor speed is as same as that of the experiment.

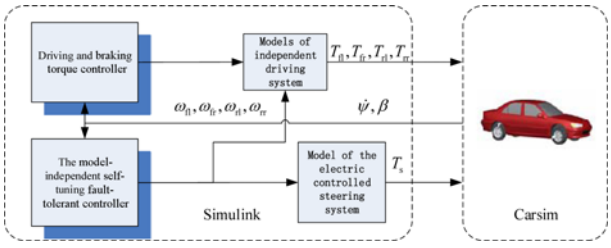

Figure 1. Structure of simulation system based on Simulink/Carsim.

Table 1. Main Parameters of the Vehicle and Actuators.

Parameter	Value
Vehicle mass (kg)	400
Sprung mass	340
Wheelbase / Track (m)	2.10 / 1.56
Front / rear axle distance to COG (m)	1.26 / 0.84
Tire radius (m)	0.28
Max. torque of Motor (N·m)	100
Max. wheel steering angle (°)	± 7

To validate the model-independent self-tuning fault-tolerant control method by the simulation, two testing conditions are used. 1) A straight uniform speed condition is selected, defined as the F1 condition: set the desired speed to 70 km/h; select drive motors failure at the same side so that the left front motor and the left rear motor become completely ineffective at the 2nd and 3rd seconds. 2) A straight acceleration condition is also selected, defined as the F2 condition: the initial speed is 70 km/h, and the desired acceleration is 0.7 m/s^2; select drive motors failure at the same side so that the left front motor and the left rear motor become completely ineffective at the 2nd and 3rd seconds.

4.1. Simulation and Analysis under F1 Condition

When the vehicle is traveling straight, if drive motor failure occurs, it will cause a reduction of the vehicle speed and may cause the departure of the vehicle from the lane. Figure 2 and Figure 3 correspond to the F1 condition under constant speed: the desired speed is 70 km/h, and the desired yaw rate is 0 °/s. At the 2nd second, left front motor failure occurs, and at the 3rd second, left rear motor failure occurs. Without control, the yaw rate error becomes larger. With control, the deviation can be corrected in a timely manner, as shown in Figure 2. For vehicle speed tracking, when motor failure occurs, the speed decreases; however, with control, the speed is corrected, whereas without control, the speed reduces continually, as shown in Figure 3.

With control, the steering motor torque immediately responds when motor failure occurs, reaching the maximum value within 0.3 s and becoming stable after 0.6 s, as shown in Figure 4. For vehicle speed tracking, the remaining motor torque is increased to compensate for the lack of drive

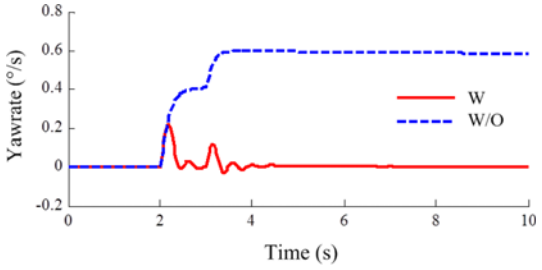

Figure 2. Yaw rate under F1 condition.

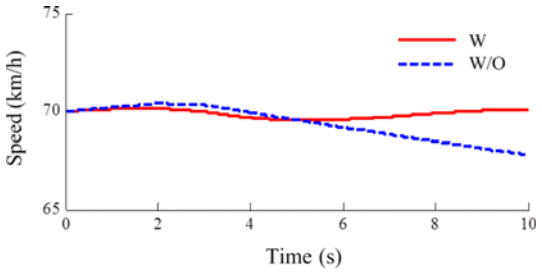

Figure 3. Vehicle speed under F1 condition.

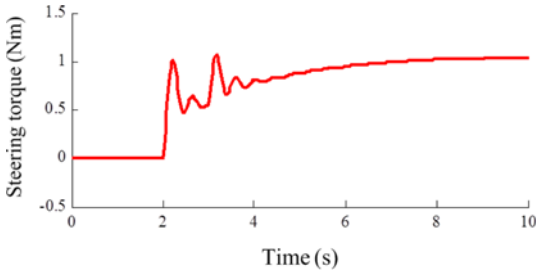

Figure 4. Steering motor torque under F1 condition.

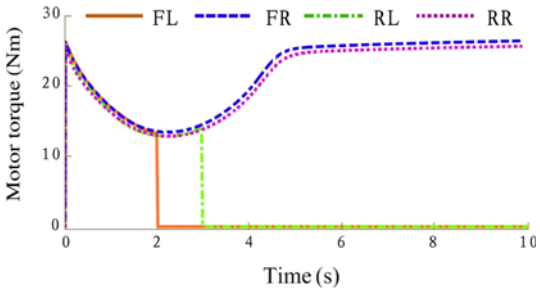

Figure 5. Driving motor torques under F1 condition.

Table 2. Statistics under F1 condition.

Item	Max. yaw rate error (°/s)	Max. speed error (km/h)
With control	0.23	0.5
Without Control	0.6	2.5

when motor failure occurs, as shown in Figure 5.

Table 2 presents the statistics under F1 condition with control and without control and provides a comparison of the results of the aspects of yaw rate errors and speed errors. With control, the maximum deviation of yaw rate is 0.23 °/s; while without control, the yaw rate deviation reaches 0.6 °/s. If the deviation is sustained, the vehicle will deviate from the intended direction. Regarding the speed, the error is 0.5 km/h with control; without control, the deviation that appears at the 10th second is 2.5 km/h, and the deviation continues to increase with time.

4.2. Simulation and Analysis under F2 Condition

Figures 6 and 7 correspond to the F2 condition under constant acceleration: the initial speed is 70 km/h, the desired acceleration is 0.7 m/s^2 and the desired yaw rate is 0 °/s. With the yaw rate response after the failure occurs, the vehicle yaw rate basically remains stables at approximately 0 °/s. Without control, the yaw rate error becomes larger, as shown in Figure 6. For vehicle speed tracking, when motor failure occurs, the speed decreases. With control, the speed is corrected, whereas without control, the speed remains almost constant, as shown in Figure 7.

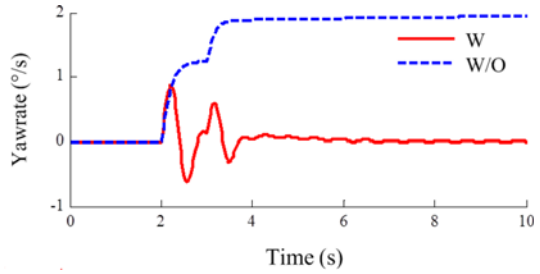

Figure 6. Yaw rate under F2 condition.

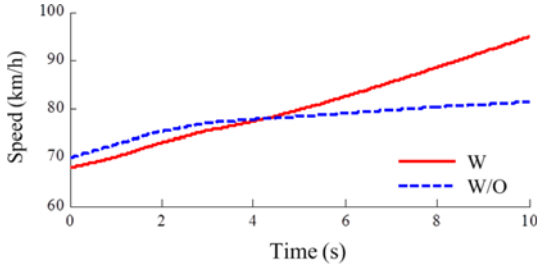

Figure 7. Vehicle speed under F2 condition.

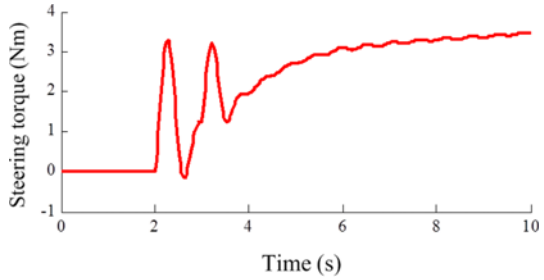

Figure 8. Steering motor torque under F2 condition.

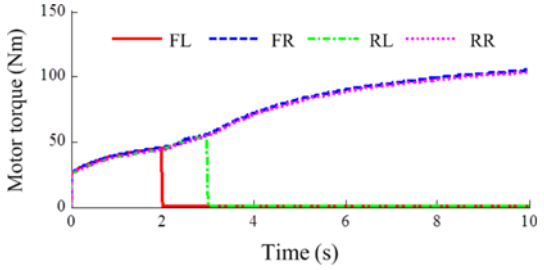

Figure 9. Driving motor torques under F2 condition.

With control, the steering torque immediately responds when motor failure occurs, reaching the maximum value within 0.3 s. Then it becomes stable after 0.8 s, as shown in Figure 8. For vehicle speed tracking, the remaining motor torque is increased to compensate the lacking drive torque when motor failure occurs, as shown in Figure 9.

Table 3 presents the statistics under F2 condition with control and without control, providing a comparison of the results of the aspects of yaw rate errors and speed errors. With control, the maximum deviation of yaw rate is 0.8 °/s; without control, the yaw rate deviation reaches 1.9 °/s.

Table 3. Statistics under F2 condition.

Item	Max. yaw rate error (°/s)	Max. speed error (km/h)
With control	0.8	2
Without Control	1.9	14

Regarding the vehicle speed, the error is 2 km/h with control; without control, the deviation that appears at the 10th second is 14 km/h.

5. EXPERIMENTS AND ANALYSIS

After the control strategy was developed, an experimental 4WID electric vehicle with the electric controlled steering system was developed by the research group, which is shown in Figure 10. The system configuration and main components of the experimental vehicle are the same as those in the simulation. The rapid control prototype of the model-independent self-tuning fault-tolerant control method is based on a MICROAUTOBOX, which has a 20 ms control period and meets the real-time requirements.

Because the prototype in-wheel motor used in the experimental vehicle works not very well, the maximum speed is just 600 rpm and the motor works very badly. So the maximum speed of the experimental vehicle is not good, the basic performances are listed in Table 4.

Figure 10. Experimental 4WID EV.

Table 4. Basic performances of the experimental vehicle.

Item	Quantity
Maximum speed	50 km/h
Acceleration time (0 km/h ~ 40 km/h)	10 s
Minimum turning radius	6 m
Max. grade ability	10 %
Driving range	50 km
Braking distance (40 km/h)	≤ 8 m
Pedal force	< 500 N

To validate the model-independent self-tuning fault-tolerant method by the experiment, two testing conditions are used. In order to compare with the simulation results, the experimental testing condition is designed almost as same as that in the simulation. Considering the performance of the prototype in-wheel motor and the safety of the experiment, two experimental testing conditions are defined. 1) A straight uniform speed condition is selected, defined as the E1 condition: set the desired speed just to 20 km/h; select drive motors failure at the same side so that the left front motor and the left rear motor become completely ineffective at the fourth seconds. 2) A straight acceleration condition is also selected, defined as the E2 condition: the initial speed is 20 km/h, and the desired acceleration is 0.2 m/s^2; select drive motors failure at the same side so that the left front motor and the left rear motor become completely ineffective at the sixth seconds.

5.1. Experiment and Analysis under E1 Condition

Figure 11 to Figure 14 corresponds to the E1 condition under constant speed: the desired speed of 20 km/h and the desired yaw rate of 0 °/s. At the fourth second, the left front and left rear motor failures occurred. Without control, the yaw rate error increased, as shown in Figure 11; with control, the deviation can be corrected in a timely manner, as shown in Figure 12. Regarding vehicle speed tracking, when the motor failure occurred, the speed decreased as shown in Figure 13; however, the speed remained constant as soon as possible under control, as shown in Figure 14.

Table 5 presents the statistics under E1 condition with control and without control, which provides a comparison of the results of the aspects of yaw rate errors and speed errors. With control, the maximum deviation of yaw rate is 0.05 °/s; without control, the yaw rate deviation reaches

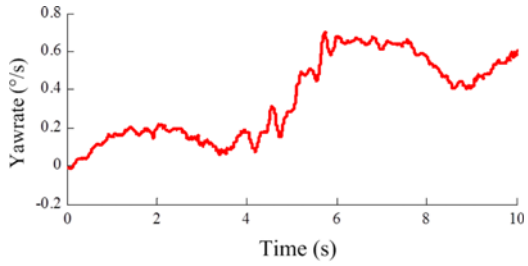

Figure 11. Yaw rate (without control) under E1 condition.

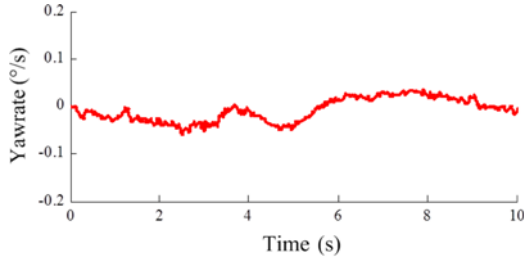

Figure 12. Yaw rate (with control) under E1 condition.

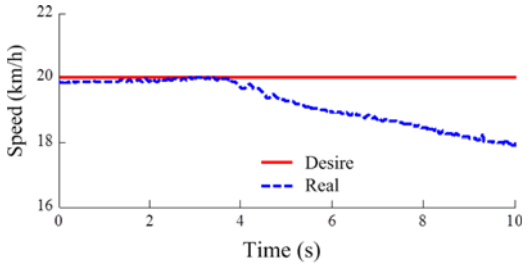

Figure 13. Vehicle speed (without control) under E1 condition.

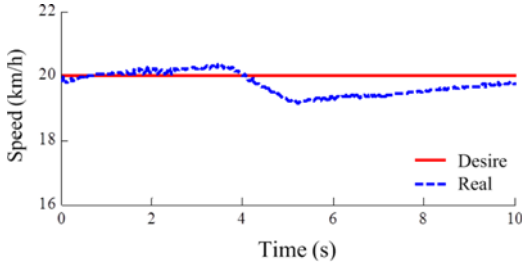

Figure 14. Vehicle speed (with control) under E1 condition.

Table 5. Statistics under E1 condition.

Item	Max. yaw rate error (°/s)	Max. speed error (km/h)
With control	0.05	0.8
Without Control	0.7	2.2

0.7 °/s, and if the deviation is sustained, the vehicle will deviate from the intended direction. Regarding the vehicle speed, with control, the maximum speed error is 0.8 km/h; without control, the deviation that appears at the 10th second is 2.2 km/h and continues to increase with time.

5.2. Experiment and Analysis under E2 Condition

Figure 15 to Figure 18 corresponds to the E2 condition under constant acceleration: the initial speed is 20 km/h, the desired acceleration is 0.2 m/s^2 and the desired yaw rate is 0 °/s. At the sixth second, motor failure occurs. With the yaw rate response (Figure 15) after the failure, the vehicle

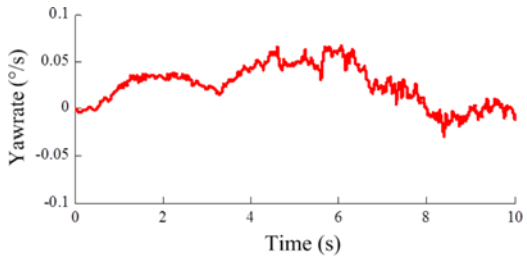

Figure 15. Yaw rate (with control) under E2 condition.

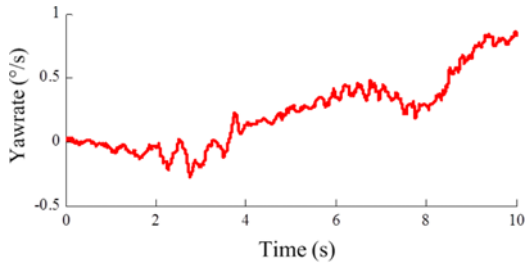

Figure 16. Yaw rate (without control) under E2 condition.

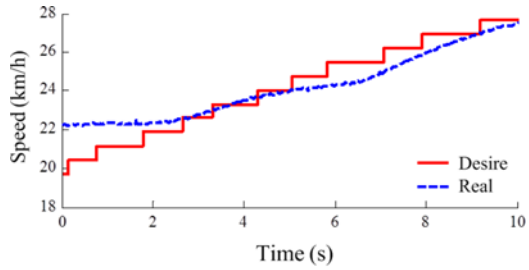

Figure 17. Vehicle speed (with control) under E2 condition.

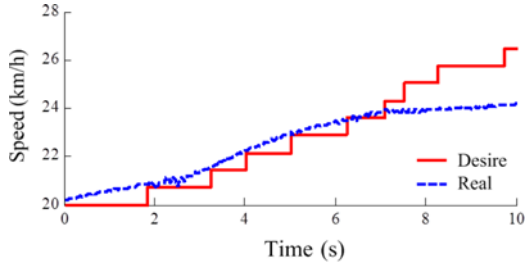

Figure 18. Vehicle speed (without control) under E2 condition.

yaw rate basically remains stable at approximately 0 °/s. Without control, the yaw rate error becomes larger, as shown in Figure 16.

Regarding vehicle speed tracking, when motor failure occurs at the sixth second, the remaining motor torque instantly increases to reach the desired acceleration, as shown in Figure 17, whereas without control, the speed reduces, as shown in Figure 18.

Table 6 presents the statistics of under E2 condition with control and without control, providing a comparison of the results of the aspects of yaw rate errors and speed errors. The controlled deviation of the yaw rate is 0.07 °/s at maximum; because the deviation and the lasting time is small, the yaw rate deviation is negligible. In addition, the

Table 6. Statistics under E2 condition.

Item	Max. yaw rate error (°/s)	Max. speed error (km/h)
With control	0.07	1.4
Without Control	0.9	3

speed error is 1.4 km/h. As a result of the control, the deviation is small and of short duration and the vehicle will not deviate from a predetermined direction. The maximum yaw rate deviation is 0.9 °/s without control and the yaw rate will always deviate from the expectations: the vehicle will deviate from the intended trajectory and the speed error is 3 km/h, which will continue to increase.

6. CONCLUSION

In this paper, a model-independent self-tuning fault-tolerant control method for a four-wheel independent drive electric vehicle with an electric controlled steering actuator was studied. When the motor fault condition is created, measurement information and error based on estimation with input constraints are used to fulfill the controller to achieve longitudinal and lateral tracking. The error convergence and bounded input and bounded output stability was demonstrated. From the simulations and experiments implemented on a prototype vehicle, the following conclusions can be made:

(1) No detailed model information is required for a model-independent self-tuning fault-tolerant controller, which simplifies the development of the controller.
(2) No fault diagnosis information is required based on the output errors, and fault-tolerant functions with robust and stable performance can still be achieved.
(3) The proposed self-tuning fault-tolerant control method can improve the vehicle safety and the longitudinal and lateral tracking ability, thereby improving vehicle fault-tolerant performance.

In the future, to improve the adaptability of the control method under different working environment, dynamic constraint of input and output will be added to the control system constraints. To furtherly test the proposed control method, curving test conditions will be considered.

ACKNOWLEDGEMENT–This research was funded by the Natural Science Foundation Project (51575295) and the National Key Fundamental Research Program of China (2011CB711204), it was supported by the Collaborative Innovation Center of Electric Vehicles in Beijing.

REFERENCES

Alwi, H. and Edwards, C. (2008). Fault tolerant control using sliding modes with on-line control allocation. *Automatica* **44**, **7**, 1859–1866.

Benbouzid, M. E. H., Diallo, D. and Zeraoulia, M. (2007). Advanced fault-tolerant control of induction-motor drives for EV/HEV traction applications: From conventional to modern and intelligent control techniques. *IEEE Trans. Vehicular Technology* **56**, **2**, 519–528.

Gadda, C. D., Laws, S. M. and Gerdes, J. C. (2007). Generating diagnostic residuals for steer-by-wire vehicles. *IEEE Trans. Control Systems Technology* **15**, **3**, 529–540.

Hess, R. A. and Wells, S. R. (2003). Sliding mode control applied to reconfigurable flight control design. *J. Guidance, Control, and Dynamics* **26**, **3**, 452–462.

Ho, L. W. and Yen, G. G. (2002). Reconfigurable control system design for fault diagnosis and accommodation. *Int. J. Neural Systems* **12**, **6**, 497–520.

Hou, Z. and Jin, S. (2011). Data-driven model-free adaptive control for a class of MIMO nonlinear discrete-time systems. *IEEE Trans. Neural Networks* **22**, **12**, 2173–2188.

Im, J. S., Ozaki, F., Yeu, T. K. and Kawaji, S. (2009). Model-based fault detection and isolation in steer-by-wire vehicle using sliding mode observer. *J. Mechanical Science and Technology* **23**, **8**, 1991–1999.

Kawakami, K., Matsugaura, S. and Onishi, M. (2001). Development of fail-safe technologies of ultra high performance EV "KAZ"[C/CD]. *The 18th Int. Battery, Hybrid and Fuel Cell Electric Vehicle Symp. & Exposition*, Berlin.

Kazemi, R. and Janbakhsh, A. A. (2010). Nonlinear adaptive sliding mode control for vehicle handling improvement via steer-by-wire. *Int. J. Automotive Technology* **11**, **3**, 345–354.

Kim, K. S., Lee, K. J. and Kim, Y. (2003). Reconfigurable flight control system design using direct adaptive method. *J. Guidance, Control, and Dynamics* **26**, **4**, 543–550.

MacKunis, W., Wilcox, Z. D., Kaiser, M. K. and Dixon, W. E. (2010). Global adaptive output feedback tracking control of an unmanned aerial vehicle. *IEEE Trans. Control Systems Technology* **18**, **6**, 1390–1397.

Plumlee, J. H. and Bevly, D. M. (2004). Control of a ground vehicle using quadratic programming based control allocation techniques. *Proc. American Control Conf.*, **5**, 4704–4709.

Polycarpou, M. M. (2001). Fault accommodation of a class of multivariable nonlinear dynamical systems using a learning approach. *IEEE Trans. Automatic Control* **46**, **5**, 736–742.

Veillette, R. J. (1995). Reliable linear-quadratic state-feedback control. *Automatica* **31**, **1**, 137–143.

Wada, N., Fujii, K. and Saeki, M. (2013). Reconfigurable fault-tolerant controller synthesis for a steer-by-wire vehicle using independently driven wheels. *Vehicle System Dynamics* **51**, **9**, 1438–1465.

Wang, J. and Longoria, R. G. (2009). Coordinated and reconfigurable vehicle dynamics control. *IEEE Trans. Control Systems Technology* **17**, **3**, 723–732.

Wang, R. and Wang, J. (2011). Fault-tolerant control with active fault diagnosis for four-wheel independently driven electric ground vehicles. *IEEE Trans. Vehicular Technology* **60**, **9**, 4276–4287.

Wang, R. and Wang, J. (2013). Passive actuator fault-tolerant control for a class of overactuated nonlinear systems and applications to electric vehicles. *IEEE Trans. Vehicular Technology* **62**, **3**, 972–985.

Widodo, A., Yang, B. S., Gu, D. S. and Choi, B. K. (2009).

Intelligent fault diagnosis system of induction motor based on transient current signal. *Mechatronics* **19**, **5**, 680–689.

Wise, K. A., Brinker, J. S., Calise, A. J., Enns, D. F., Elgersma, M. R. and Voulgaris, P. (1999). Direct adaptive reconfigurable flight control for a tailless advanced fighter aircraft. *Int. J. Robust and Nonlinear Control* **9**, **14**, 999–1012.

Yang, G. H., Wang, J. L. and Soh, Y. C. (2000). Reliable LQG control with sensor failures. *IEE Proc. Control Theory and Applications* **147**, **4**, 433–439.

Yim, S. (2014). Fault-tolerant yaw moment control with steer and brake-by-wire devices. *Int. J. Automotive Technology* **15**, **3**, 463–468.

Zidani, F., Benbouzid, M. E. H., Diallo, D. and Benchaib, A. (2003). Active fault-tolerant control of induction motor drives in EV and HEV against sensor failures using a fuzzy decision system. *Electric Machines and Drives Conf., IEMDC'03. IEEE Int.,* **2**, 677–683.